

# Backstepping approach and Bio Inspired model based hybrid sliding-mode tracking control for Airship

Tami Y. <sup>1</sup>Melbous A. <sup>2</sup>Guessoum A. <sup>3</sup>

<sup>1,2,3</sup> Laboratory of Electric System and Remote Control, Electronic Department  
University Saad Dahleb Blida (Algeria)

tami.youcef@yahoo.fr

melbsaek@yahoo.com

guessouma@hotmail.com

**Abstract** : A novel hybrid control approach is presented for trajectory tracking control of an autonomous airship vehicles in this paper. The kinematic and dynamic controllers are integrated by the proposed control strategy. The paper has two objectives. Firstly, an improved backstep method is proposed to generate the virtual velocity using a bio-inspired neurodynamics model in the kinematic controller.

The bio-inspired neurodynamics model is intended to smooth the virtual velocity output to avoid speed jumps of the autonomous airship vehicle caused by tracking errors. Secondly, a new sliding-mode method is added to the dynamic controller, which is robust against parameter inaccuracy and disturbances. The combined kinematic–dynamic control law is applied to the trajectory tracking problem of an autonomous airship vehicle. Finally, simulation results illustrate the performance of the proposed controller.

**Keywords** : autonomous airship vehicle, Tracking control, Biological inspired neurodynamics, Backstepping control, Sliding mode control.

## 1. INTRODUCTION

As a typical lighter-than-air (LTA) vehicle, the autonomous airship is a unique and promising platform for many different kinds of applications, such as telecommunication, broadcasting relays, disaster guard, and scientific exploration (Schafer and Reimund, 2002; Chu and Blackmore, 2007; Yang *et al.* 2012). With the rapid progress of airship technologies, the advanced flight control system plays a key role in the development of the autonomous airship. Nonlinear dynamics, model uncertainties, and external disturbances contribute to the difficulty in maneuvering an airship to track a time-varying reference trajectory. Therefore, trajectory tracking control remains a key technical challenge for the autonomous airship (Yang *et al.* 2011b) [3].

The autonomous airship vehicle dynamics is strongly coupled and highly nonlinear. In order to deal with the uncertain nonlinear parts in the autonomous airship vehicle's dynamics, many researchers concentrated their interests on the applications of sliding mode control. Sliding mode method [3] is usually used for dynamic tracking control for the outstanding characteristic including

insensitivity to parameter variations, and good rejection of disturbances. So Sliding mode control is extraordinary suitable for robust tracking control of autonomous airship vehicle. However, one major drawback of the sliding-mode approach is the high frequency of control action (chattering). To eliminate/reduce chattering, various methods have been proposed to reach a continuous robust control. For example, S. Serdar proposed a chattering-free sliding-mode control method with an adaptive estimate term [3].

The backstepping control algorithm is the commonly used approach for tracking control. However, the disadvantage for backstepping method is quite obvious [4]. The velocity control law is directly related to the state errors, so large velocities will be generated in big initial error condition and sharp speed jump occurs while sudden tracking error happens.

It means that the required acceleration and forces/moments exceed their control constraint even infinite values at the velocity jump points, which is practically impossible.

Several control approaches have been proposed for the trajectory tracking of an airship in the literature. Moutinho and Azinheira (2005) designed the longitudinal and lateral control system of the AURORA airship using the dynamic inversion control method. This control system has limitations because it was developed based on the linear model, neglecting dynamic nonlinearity and coupling effects between longitudinal and lateral motions. *Filoktimon* and *Evangelos* (2008) proposed a backstepping control approach for trajectory tracking of a robotic airship. *Lee* and *Rendon* designed a backstepping design formulation for trajectory control of an unmanned airship (*Lee and Lee, 2007; Murguia-Rendon et al. 2009*). The design of a backstepping control system should follow the exact model. However, the airship model always has uncertainties, and the model parameters are difficult to estimate accurately in an operational situation. Each method has its advantage and disadvantage, it is difficult to use a single method to deal with all the problems.

In this paper, for the problems of speed jumps control constraints, we present a kinematics/dynamics control system based on a velocity controller with biological neurons and an sliding mode controller. The simulation

studies have verified that the proposed control system is able to realize the real-time dynamic tracking of airship and has better performance than the traditional backstepping method.

The paper is structured as following parts. After a brief description of the dynamic control strategy and the existing problems in *Section 1*, the horizontal kinematic and dynamic models of autonomous airship are introduced in *Section 2*, which followed by description of backstepping path-following control strategy. In *Section 3*, the hybrid control strategy based on a biological inspired model and a backstepping method is presented. In *Section 4*, simulation and experimental comparison, including a circle and a line followed by the autonomous airship. The results have verified that the proposed control method is effective. Section 5 contains the conclusion of the work.

## 2. Kinematic and Dynamic Models

### 2.1 Kinematic model

The two coordinate frame systems for the autonomous airship are illustrated in *Fig. 1* including the inertial frame system  $\{O_e - X_e Y_e Z_e\}$  and the body-fixed frame system  $\{O_b - x_b y_b z_b\}$  in a three-dimensional Cartesian workspace. The kinematic model of the autonomous airship can be expressed as follows: [1]

$$\dot{\eta} = J(\eta)q \quad (1)$$

where  $\eta = [x \ y \ z \ \phi \ \theta \ \psi]^T$  represents the position and the orientation with respect to the inertial frame;  $q = [u \ v \ w \ p \ q \ r]^T$  is the translational and angular velocities vector with respect to the body-fixed frame;  $J \in R^{6 \times 6}$  is the spatial transformation matrix between the inertial frame and body-fixed frame.

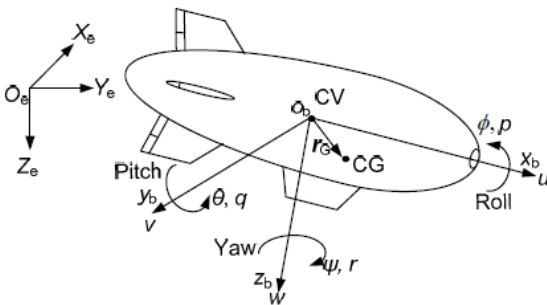


Fig. 1: Position of frames

### 2.2 Dynamic model

The dynamic model of an autonomous airship can be expressed as a compact equation: [7]

$$M\dot{q} + C(q)q + D(q)q + g(\eta) = \tau \quad (2)$$

Where  $M \in R^{6 \times 6}$  is the inertial matrix including the added mass;  $C(q) \in R^{6 \times 6}$  denotes the matrix of Coriolis and centrifugal forces including added mass;  $D(q) \in R^{6 \times 6}$  is the damping matrix;  $g(\eta) \in R^6$  represents the vector of gravity and buoyancy forces and moments;  $\tau \in R^6$  is the control forces and moments.

In this paper, only four degrees of freedom, i.e.,  $p = q = 0$ , are considered due to the complexity of the system and the fact they describe well main characteristics of the overall system. Hence, the above-mentioned matrices can be simplified as

$$\eta = [x \ y \ z \ \psi]^T \in R^4$$

$$q = [u \ v \ w \ r]^T \in R^4, \quad J \in R^{4 \times 4}, \quad M \in R^{4 \times 4}, \\ C(q) \in R^{4 \times 4}, \quad D(q) \in R^{4 \times 4}, \quad g(\eta) \in R^{4 \times 4}.$$

$$J = \begin{bmatrix} J_{11} & J_{12} & 0 & 0 \\ J_{21} & J_{22} & 0 & 0 \\ 0 & 0 & J_{33} & 0 \\ 0 & 0 & 0 & J_{44} \end{bmatrix},$$

$$J_{11} = \cos \psi, \quad J_{12} = -\sin \psi, \quad J_{21} = \sin \psi, \quad J_{22} = \cos \psi, \\ J_{33} = 1, \quad J_{44} = 1;$$

$$M = \begin{bmatrix} m_{11} & 0 & 0 & 0 \\ 0 & m_{22} & 0 & 0 \\ 0 & 0 & m_{33} & 0 \\ 0 & 0 & 0 & m_{44} \end{bmatrix},$$

$$m_{11} = m - X_{ii}, \quad m_{22} = m - Y_{vv}, \quad m_{33} = m - Z_{ww}, \\ m_{44} = I_z - N_{rr};$$

$$C(q) = \begin{bmatrix} 0 & 0 & 0 & c_{14} \\ 0 & 0 & 0 & c_{24} \\ 0 & 0 & 0 & 0 \\ c_{41} & c_{42} & 0 & 0 \end{bmatrix},$$

$$c_{14} = -(m - Y_{vv})v, \quad c_{24} = (m - X_{ii})u, \quad c_{41} = (m - Y_{vv})v, \\ c_{42} = -(m - X_{ii})u;$$

$$D = \begin{bmatrix} d_{11} & 0 & 0 & 0 \\ 0 & d_{22} & 0 & 0 \\ 0 & 0 & d_{33} & 0 \\ 0 & 0 & 0 & d_{44} \end{bmatrix},$$

$$d_{11} = -X_{uu}, \quad d_{22} = -Y_{vv}, \quad d_{33} = -Z_{ww}, \quad d_{44} = -N_{rr};$$

where  $m$  is the mass of the airship;  $I_z$  denotes the moment of inertia with respect to  $z$  axis;

$X_{ii}, Y_v, Z_w, N_r$  and  $X_u, Y_v, Z_w, N_r$  are the added inertial parameters.

### 2.3 Tracking control problem

The autonomous airship is usually required to move at a low forward speed and a low rotational speed when it executes investigation tasks. This needs a precious tracking control. Consider that the autonomous airship major movement is in four degrees of freedom (DOF): surge, sway, heave, yaw, so in this paper, only the four DOF tracking control problem is represented. The controller design problem can be described as follows. The desired state of the autonomous airship is defined as

$$\eta_d = [x_d \ y_d \ z_d \ \psi_d]^T \quad (3)$$

Where  $\eta_d = [x_d \ y_d \ z_d \ \psi_d]^T$  the desired state of autonomous airship in the inertial frame is,  $(x_d \ y_d \ z_d)$  is coordinate of desired path in the inertial frame,  $\psi_d$  is the counter-clockwise rotation angle of airship along the Z-axis.

The desired forward and angular velocities can be deduced By : [5] [6]

$$u_d = \dot{x}_d \cos \psi_d + \dot{y}_d \sin \psi_d$$

$$v_d = \dot{x}_d (-\sin \psi_d) + \dot{y}_d \cos \psi_d$$

$$w_d = \dot{z}_d$$

$$r_d = \dot{\psi}_d = \frac{\dot{x}_d \dot{y}_d - \dot{x}_d \dot{y}_d}{\dot{x}_d^2 + \dot{y}_d^2}$$

The actual state of airship is represented by:

$$\eta = [x \ y \ z \ \psi]^T, \quad q = [u \ v \ w \ r]^T.$$

As the objective of the path tracking controllers is to make airship follow the known path by controlling the velocity and angular velocities, so the tracking error  $e = \eta_d - \eta = [e_x \ e_y \ e_z \ e_\psi]^T$  converges to zero. Here  $e$  is the tracking error in the inertial frame. A detailed model of tracking control problem is given in Fig. 2.

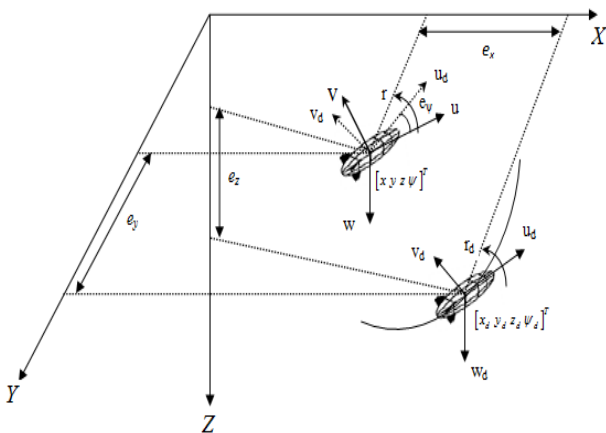


Fig. 2 Tracking control problem

### 3. CONTROL ALGORITHMS

The basic control architecture of the system is illustrated in Fig. 3. The design of the hybrid control strategy consists of two parts: (1). an outer loop virtual velocity controller by using position and orientation state errors; (2). an inner loop sliding-mode controller by using velocity state vector.

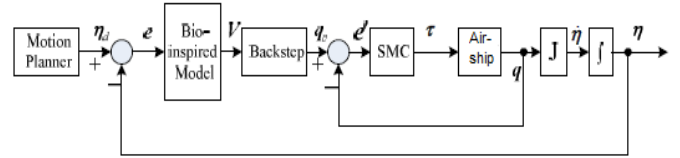


Fig. 3 The cascaded controller of Airship.

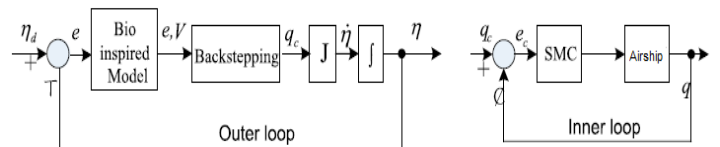


Fig. 4 The separated two closed loops

#### 3.1. Virtual velocity controller

Backstepping method for nonholonomic mobile robot has been designed a lot for velocity tracking [4] [7] [9]. But the autonomous airship in this study is a holonomic system, so the backstepping control law for the mobile robot is not fit for this control system. For this reason, a new backstepping control law is designed for UAV and makes it possible to follow a given reference posture with stability.

The virtual velocity controller based on the backstepping approach can be defined as:

$$q_c = \begin{bmatrix} u_c \\ v_c \\ w_c \\ r_c \end{bmatrix} = \begin{bmatrix} k(e_x \cos \psi + e_y \sin \psi) + (u_d \cos e_\psi - v_d \sin e_\psi) \\ k(-e_x \sin \psi + e_y \cos \psi) + (u_d \sin e_\psi + v_d \cos e_\psi) \\ w_d + k_z e_z \\ r_d + k_\psi e_\psi \end{bmatrix} \quad (12)$$

Where  $k, k_z, k_\psi$  are constant coefficients,

$q_d = [u_d \ v_d \ w_d \ r_d]^T$  is the desired velocity in the body-fixed frame,  $u_d \cos e_\psi - v_d \sin e_\psi$  and  $u_d \sin e_\psi + v_d \cos e_\psi$  represents the desired velocity frame transformed to the actual velocity frame seen in figure. 2.

#### 3.2. Bio-inspired velocity controller

Bio-inspired model was first proposed by Grossberg from the current mechanism using circuit element to simulate the cell membranes throught up by Hodkin and Huxley. The dynamic characteristics of the membrane voltage on the film can be described by the following state equation [4] [7] [9]:

$$C_m \frac{dV_m}{dt} = -(E_p + V_m)g_p + (E_{Na} - V_m)g_{Na} - (E_K + V_m)g_K$$

Where  $C_m$  represents membrane capacitance;  $E_K$ ,  $E_{Na}$  and  $E_p$  represent the resting potentials in the membrane respectively;  $g_K$ ,  $g_{Na}$  and  $g_p$  represent the admittance coefficients respectively.

By setting  $V = E_p + V_m$ ,  $A = g_p$ ,  $B = E_{Na} + E_p$ ,  $C_m = 1$ ,  $D = E_K - E_p$ ,  $S(t)^+ = g_{Na}$ ,  $S(t)^- = g_K$ ,

The bio-inspired model can be simplified into :

$$\frac{dV}{dt} = -AV + (B - V)S(t)^+ - (D + V)S(t)^-$$

Note that  $V$  is the neural activity of the neuron.

The parameters  $A$ ,  $B$  and  $D$  are the nonnegative constants describing the passive decay rate, the upper and lower bounds of the neural activity value respectively. The variables  $S^+(t)$  and  $S^-(t)$  represent the excitatory and inhibitory input to a neuron, respectively. The shunting dynamic of an individual neuron can be modeled by this equation. The state responses of the models are limited to the finite interval  $[-D, B]$  because of the auto gain-regulation of the model. So we can infer the shunting equation to the following form:

$$\dot{V}_i = -AV_i + (B - V_i)f(e_i) - (D + V_i)g(e_i)$$

Where  $i$  is the neuron index,  $f(e_i) = \max(e_i, 0)$ ,

$$g(e_i) = \max(-e_i, 0).$$

It is guaranteed that the neural activity will stay in this Interval for any value of the excitatory and inhibitory inputs. It is continuous and smooth. We put biological neurons model to the traditional velocity controller, so the equation (12) can be written as:

$$q_c = \begin{bmatrix} u_c \\ v_c \\ w_c \\ r_c \end{bmatrix} = \begin{bmatrix} k(V_x \cos \psi + V_y \sin \psi) + (u_d \cos e_\psi - v_d \sin e_\psi) \\ k(-V_x \sin \psi + V_y \cos \psi) + (u_d \sin e_\psi + v_d \cos e_\psi) \\ w_d + k_z V_z \\ r_d + k_\psi V_\psi \end{bmatrix} \quad (14)$$

Where  $V_i$  ( $i = x, y, z, \psi$ ) represent the outputs of the biological neurons model.

### 3.3 Sliding mode control :

After the velocity controller generates the virtual velocity of the autonomous airship, a sliding-mode controller is used to generate the control forces and moments  $\tau = [\tau_x \quad \tau_y \quad \tau_z \quad \tau_N]^T$ . Then the control inputs  $\tau$  will be applied to the autonomous airship

dynamic model to produce the actual velocity in surge, sway, heave and yaw ( $q = [u \quad v \quad w \quad r]^T$ ) in the

body-fixed frame respectively. So it will be easy to get the actual airship vehicle's states ( $\eta = [x \quad y \quad z \quad \psi]^T$ ) in the inertial frame by  $\dot{\eta} = Jq$ . As a rule, sliding-mode control can be divided into two parts. First, define a sliding manifold  $s$ . Second, find a control law to move toward the sliding manifold. The sliding manifold is defined as [8] :

$$s = \dot{e}_c + 2\Lambda e_c \quad (15)$$

Where  $e_c = q_c - q$  is the velocity error between the virtual velocity and the actual velocity,  $\Lambda$  represents a strictly positive constant,  $s$  is a 4x1 vector. Derivation of (15), then

$$\dot{s} = \ddot{e}_c + 2\Lambda \dot{e}_c = \ddot{e}_c + 2\Lambda(\dot{q}_c - \dot{q}) \quad (16)$$

When the system is operating on the sliding surface, (16) equals zero, i.e.

$$\dot{s} = \ddot{e}_c + 2\Lambda \dot{e}_c = \ddot{e}_c + 2\Lambda(\dot{q}_c - \dot{q}) = 0 \quad (17)$$

We put equation (2) into equation (17), then

$$\ddot{e}_c + 2\Lambda(\dot{q}_c - M^{-1}(\tau - Cq - Dq - g)) = 0 \quad (18)$$

So the equivalent control law can be concluded as

$$\tau_{eq} = \hat{M} \left( \dot{q}_c + \frac{\ddot{e}_c}{2\Lambda} \right) + \hat{C}q + \hat{D}q + \hat{g} \quad (19)$$

where,  $\hat{M}$ ,  $\hat{C}$ ,  $\hat{D}$ ,  $\hat{g}$  are estimated terms. Considering the difficulty of computing  $\ddot{e}_c$  in (19), a feedback control input of acceleration error is introduced

$$\ddot{e}_c = -k\dot{e}_c \quad (20)$$

Where  $k$  is a constant scalar representing the strictly positive constant that determines the rate of acceleration error. The conventional sliding-mode can be designed as

$$\tau = \tau_{eq} + k \operatorname{sgn}(s) \quad (21)$$

## 4. SIMULATION

In this paper, two methods were simulated for trajectory tracking problem: the proposed backstepping controller and the bio-inspired controller. The backstepping method given in Eq. (12) was used as a case study to illustrate the performance of the proposed control strategies. The aim of the simulation is to illustrate the

advantages of the proposed controller in driving an airship vehicle on to a desired trajectory.

The control system was simulated using the variable step Runge-Kutta integrator in MATLAB. The model parameters of the airship [3] are given in Table 2.

**Table 2: Model parameters of the airship**

Parameter	Value	Parameter	Value
m (kg)	239	$X_u$ (kg)	-4.235
$X_u$ (kg)	216.7	$Y_v$ (kg)	-21.668
$Y_v$ (kg)	215	$Z_w$ (kg)	-21.668
$Z_w$ (kg)	215	$N_r$ (kg)	-3.423
$N_r$ (kg)	50.2	$I_z$ (kg.m <sup>2</sup> )	12826.7

### 4.1 Straight line trajectory tracking

A simple case to track a straight line was studied first. The horizontal state vector of autonomous airship is  $\eta = [x(t) \ y(t) \ z(t) \ \psi(t)]^T$  where t represents the simulation time. Assume that the desired state of airship is:  $x_d(t) = 5 + 0.5t$ ,  $y_d(t) = 0.5t$ ,  $z_d(t) = 0.01t$ ,  $\psi_d(t) = 0.01$  and the actual initial state is  $\eta(0) = [x(0) \ y(0) \ z(0) \ \psi(0)]^T = [0 \ 0 \ 0 \ 0]^T$ . The parameter settings of the hybrid controller are presented in tables 3. The parameters in Tables 3 were obtained through several simulation results.

**Table 3: the controller parameters (Airship).**

K	$\Lambda$	k	$K_\psi$	$K_z$	A	B	D
600	2	2	1	2	5	10	10

For the backstepping method (non-biological inspired), the virtual velocity controller  $q_c$  can be calculated by Eq. (12); For the biological inspired, the virtual velocity controller  $q_c$  can be calculated by Eq. (14); Then by using the virtual velocity controller  $q_c$ , a sliding-mode controller Eq. (21) is used to generate the control forces and moments  $\tau$ . The simulation results for trajectory tracking are shown in Fig.4. It takes a short time to catch up and land on the desired path smoothly for two kinds of methods, but their velocity responses are obviously different from each other. For the controller based on the backstepping approach, this controller occurs the sharp speed jumps when tracking errors change suddenly at initial time.

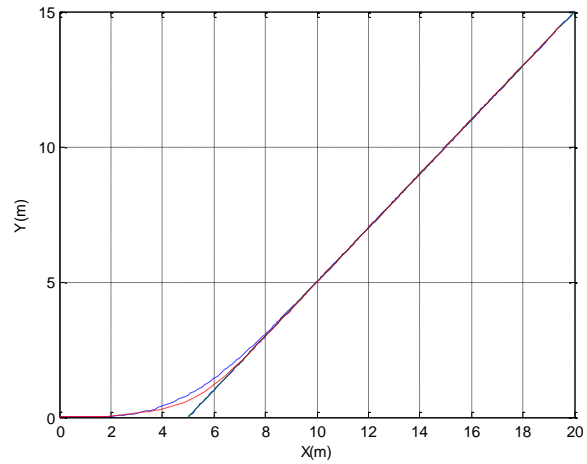


**Fig. 5 Trajectories using bio-inspired model (bleue dotted line) and backstepping method (red solid line).**

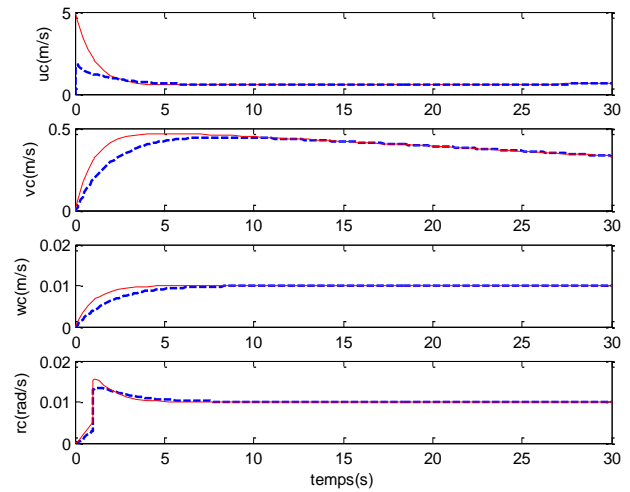


**Fig. 6 Virtual velocity using bio-inspired model (blue dotted line) and the backstepping method (red solid line).**

For example, the virtual surge speed of the backstep method jumps to more than 5 m/s whereas the value for the biological inspired method is 2 m/s (Fig.5). It seems that the backstep method (red solid line) exhibits good performance because the vehicle reaches the straight-line trajectory quickly.

### 4.2 Circular trajectory tracking

Considering that the turning circle maneuver is an important practical trajectory maneuver that the airship needs to perform frequently, we examine the control performance of circle trajectory tracking using the designed control scheme. The desired trajectory is generated using the following command generator:

$$\dot{x}_d = 5 \cos(0.01t) ; \dot{y}_d = 5 \sin(0.01t) ; \dot{z}_d = 0.01 ; \dot{\psi}_d = 0.01$$

$$v_d = [u_d \ v_d \ w_d \ r_d]^T = [5 \text{ m/s}, 0 \text{ m/s}, 0 \text{ m/s}, 0.01 \text{ rad/s}]^T$$

and the initial state of the airship was set to be:

$$\eta_0 = [x_0 \ y_0 \ z_0 \ \psi_0]^T = [500 \text{ m}, 500 \text{ m}, 0, -\pi/2]^T$$

Simulation results were obtained for two cases: (1) the model parameters are known and (2) there are parameter uncertainties and external disturbances.

**Case 1:** The following simulations concern the trajectory tracking control design based on the accurate model parameters. The parameter setting of the hybrid controller is the same as for the simulation of straight-line tracking. The simulation results of trajectory tracking are shown in **fig.6**. Both simulation results show satisfactory behavior of the airship. It can be seen from Fig 6. The airship takes some time to reach and stay on the desired path for both track control procedures. However, the virtual velocity responses (linear and angular velocities in Fig. 7) are different for the two different velocity controllers.

The virtual velocity based on the backstep approach exhibits sharp speed jumps when the tracking errors change suddenly at the initial time; For example, the virtual sway speed (**vc**) of the backstep method jumps to more than **1000 m/s**, whereas this value for the bio-inspired method is about **50 m/s** in Fig.7.

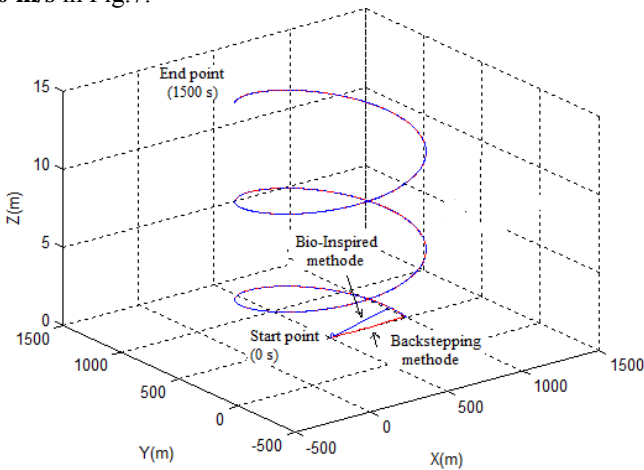


**Fig. 7** Systems trajectories using bio-inspired model (blue line) and the backstepping method (red line).

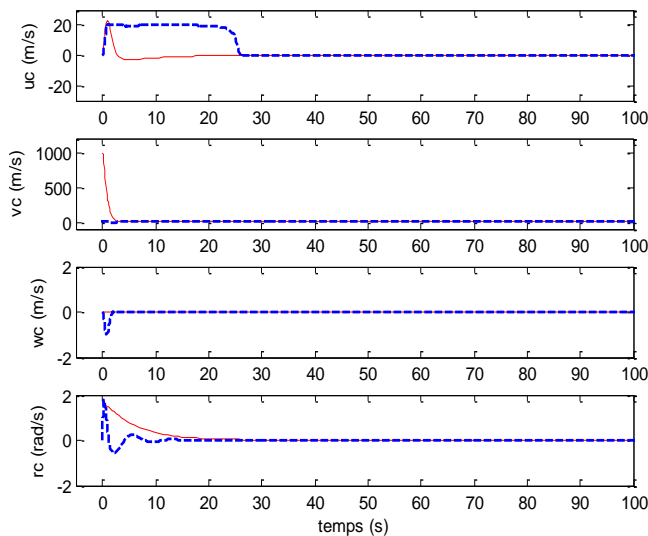


**Fig. 8** Virtual velocity using bio-inspired model (blue dotted line) and the backstepping method (red solid line).

In addition, From **Fig. 6** (the simulation result of Trajectory tracking), **Fig.7** (virtual velocity), it can be seen that the proposed control method is chattering free and robust against dynamic uncertainties and disturbances, due to the use of the sliding-mode algorithm in the hybrid controller.

While all the work in this paper is based on numerical simulation and analysis, our major contribution is the application of the bio-inspired neurodynamics model. Our main idea is that the bio-inspired neurodynamics model can address the sharp speed jumps seen when using the backstep method, and that a smooth and physically realizable control signal is generated without any limitation, which cannot be achieved using the backstep method.

**Case 2:** We concern the robustness properties of the designed control scheme to parameter uncertainties and external disturbances. We conducted simulations in which errors of the order of **5%** on all parameters in Table 2 were assumed [ ]. In practice, the external disturbances mainly may be the wind disturbances.

We assume that the wind disturbances in the lateral direction are  $dw = 10 \cos t \text{ m/s}$ , where **10 m/s** is the wind velocity; that is, wind disturbances vary in form of a cosine function with a magnitude of **10 m/s**.

Simulation results concerning the inaccurate model parameters and wind disturbance are shown in **Figs.9** and **10**.

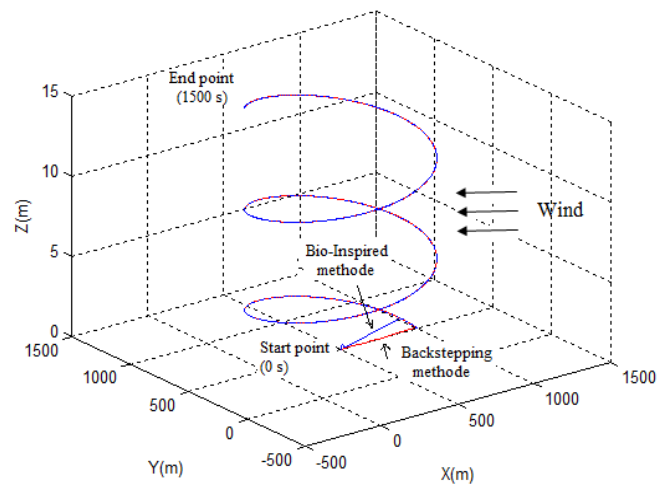


**Fig. 9** Systems trajectories using bio-inspired model (blue line) and the backstepping method (red line) with inaccurate parameters and disturbances.

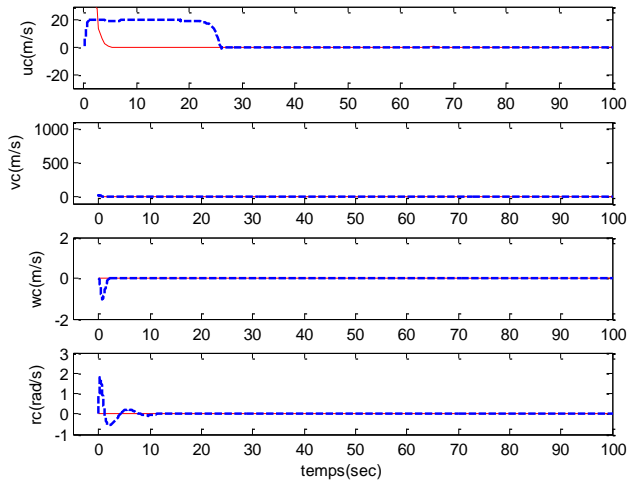


**Fig. 10** Virtual velocity using bio-inspired model (blue dotted line) and the backstepping method (red solid line) with inaccurate parameters and disturbances.

**Fig.9** end **Fig.10** presents the simulation results of circle trajectory tracking and virtual velocity with inaccurate parameters and wind disturbances. The red solid line represents the trajectory using Backstepping method, whereas the blue dotted line represents the trajectory using Bio-inspired method. From **Fig.9**, we conclude that the proposed control scheme can track the desired trajectory accurately despite parameter uncertainties and external disturbances.

### 4.3 Curve Path Tracking

The main research in this paper is focused on continuous trajectory, which means that the trajectory is continuous and differentiable. The main problem is the initial state errors that cause the sharp speed jumps. The Airship starts at posture  $(5, 0, 0, 0)$ , while the desired initial posture is  $(0, 0, 0, 0)$ . Time varies from 0 to 35 s. Assume that the desired track state of the Airship

$$\text{is: } x_d(t) = 0.5t, y_d(t) = 0.5t + \sin(0.25t),$$

$$z_d(t) = 0.2t \text{ and } \psi_d(t) = a \tan 2(\dot{y}_d(t) / \dot{x}_d(t)).$$

The parameter setting of the cascaded controller is shown in **Table 4**.

K	$\Lambda$	k	$K_\psi$	$K_z$	A	B	D
600	2	2	1	2	10	5	5

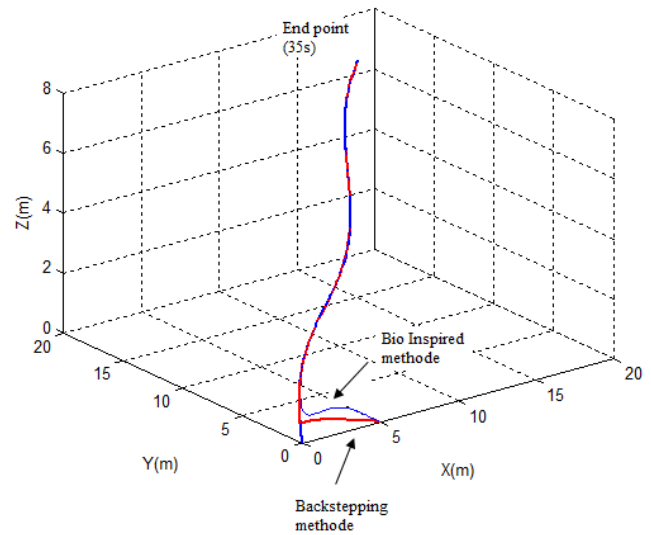


**Fig. 10** Systems trajectories using bio-inspired model (blue line) and the backstepping method (red line).

**Figs. 10** and **11** show the simulation results of the curve tracking. The red solid lines indicate the backstepping method results, and the blue solid lines are the bioinspired method results.

**Figs. 10** and **11** show the tracking control results and velocity  $q_c$  of the backstepping method and the bioinspired method, respectively.

In **Fig. 10**, the two kinds of methods can all catch up and land on the desired path smoothly.

As can be seen in **FIG. 11**, the auxiliary velocity terms (linear and angular velocities) with the bioinspired model are smoother than with the backstepping model and show a less sharp jumps. For example, the auxiliary surge speed  $uc$  of the backstepping method jumps to about  $-8 \text{ m/s}$  in the initial point, but the bioinspired method is less than  $-1 \text{ m/s}$  in **Fig.11**.

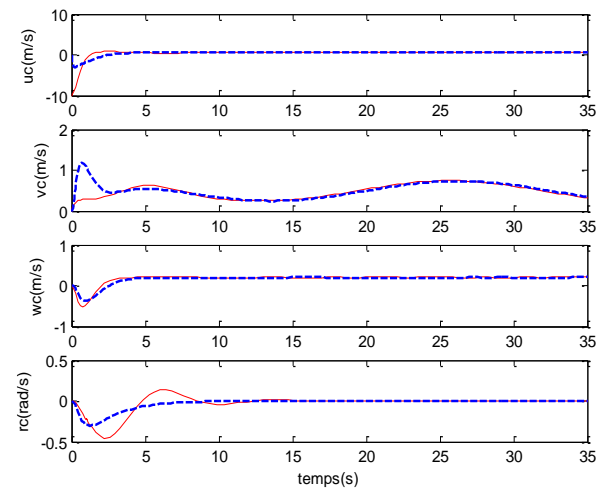


**Fig. 11** Virtual velocity using bio-inspired model (blue dotted line) and the backstepping method (red solid line).

## 5. CONCLUSION

Background information about tracking control of airship is firstly established in the paper. Then a backstepping and sliding mode tracking control algorithm is proposed for three-dimensional tracking control problem. In the control system, there exist two closed loop systems: inner loop ensures the velocity tracking and the outer loop ensures the position and orientation tracking. In the traditional backstepping method, it always suffers from the sharp speed jump problem. Because of the smooth and bounded response properties, the proposed velocity controller uses the bio inspired model to eliminate or inhibit the sharp speed jumps. From the simulation results, it is clearly to see bio-inspired method reduces the sharp speed jumps without significant performance loss while the conventional backstepping method may cause sharp speed jump problem.

## REFERENCES

- [1] Melbous A, Tami. Y, Guessoum. A, “**UAV Controller Design and Analysis using Sliding Mode Control.**” 3rd International Conference on Electrical Engineering Design and Technologies Oct. 31 – Nov. 02, 2009 Sousse, Tunisia
- [2] Bing Sun, Daqi Zhu, and Simon X. Yang, “**A Bioinspired Filtered Backstepping Tracking Control of 7000-m Manned Submarine Vehicle**”, IEEE TRANSACTIONS ON Industrial Electronics, Vol. 61, NO. 7, JULY 2014.
- [3] Yue-neng YANG, Jie WU, Wei ZHENG, “**Trajectory tracking for an autonomous airship using fuzzy adaptive sliding mode control.**”, Yang et al. / J Zhejiang Univ-Sci C (Comput & Electron) 2012 13(7):534-543.
- [4] Daqi Zhu, Yue Zhao, and Mingzhong Yan, “**A Bio-Inspired neurodynamics based Backstepping path following control of an AUV with ocean current**”, International Journal of Robotics and Automation, Vol. 27, No. 3, 2012.
- [5] Xun Hua, Daqi Zhu and Xiang Cao, “**A neurodynamics control strategy for real-time tracking control of autonomous underwater vehicle.**” 2013 25th Chinese Control and Decision Conference (CCDC).
- [6] Bing Sun, Daqi Zhu ,Feng Ding , Simon X. Yang,” **A novel tracking control approach for unmanned underwater vehicles based on bio-inspired neurodynamics**”, J Mar Sci Technol (2013) 18:63–74.
- [7] Bing Sun, Daqi Zhu, Weichong Li,” **An Integrated Backstepping and Sliding Mode Tracking Control Algorithm for Unmanned Underwater Vehicles**”, UKACC International Conference on Control 2012 Cardiff, UK, 3-5 September 2012.
- [8] Filoktimon Repoulas and Evangelos Papadopoulos, “**Robotic Airship Trajectory Tracking Control Using a Backstepping Methodology**”, 2008 IEEE International Conference on Robotics and Automation Pasadena, CA, USA, May 19-23, 2008.
- [9] Daqi Zhu, BingSun, “**The bio-inspired model based hybrid sliding-mode tracking control for unmanned underwater vehicles**”, Engineering Applications of Artificial Intelligence 26 (2013) 2260–2269.
- [10] L. BEJI and A. ABICHOU. “**Tracking control of trim trajectories of a blimp for ascent and descent flight manoeuvres**”, International Journal of Control Vol. 78, No. 10, 10 July 2005, 706–719.
- [11] J. Wang, J. Chen, S. Ouyang, Y. Yang, “**Trajectory tracking control based on adaptive neural dynamics for four wheel drive omnidirectional mobile robots.**” Engineering Review, Vol. 34, Issue 3, 235-243, 2014.